Determination of the diastereomeric excesses of chiral flavonoids in organs of *Citrus aurantium* with two-dimensional supercritical fluid chromatography

Laurine Réset, Bibi Ousseni, Laëtitia Fougère, Christophe Hano, Clément de Saint Jores, Caroline West

Determination of the diastereomeric excesses of chiral flavonoids in organs of *Citrus aurantium* with two-dimensional supercritical fluid chromatography

Laurine Réset, Bibi Ousseni, Laëtitia Fougère, Christophe Hano, Clément De Saint Jores, Caroline West*

Université d'Orléans, CNRS, ICOA, UMR 7311, Orléans, France

Corresponding Author

Caroline West - University of Orleans, ICOA, CNRS UMR7311, Pôle de chimie, rue de Chartres - BP 6759 45067, Orléans Cedex 2, France

orcid.org/0000-0001-7595-6777

Phone: +33 2 38 49 47 78

e-mail: caroline.west@univ-orleans.fr

Abstract

Citrus aurantium (bitter orange), is widely used in culinary preparations, food supplements, cosmetics and traditional medicine. Its bioactivity is mainly associated to two major flavonoids, naringin and neohesperidin, which are chiral glycosylated flavanones, each comprising two diastereoisomers having different bioactivities, like bitterness.

A two-dimensional supercritical fluid chromatography method was used to measure diastereomeric excesses of the flavonoids in bitter orange organs, including flowers, leaves of different origin, fruits at different stages of maturity and dried with different drying methods. The extracts were prepared with supercritical fluid extraction (SFE) with CO_2, ethanol and water. SFE conditions were defined following a 3-factor Box-Behnken design of experiments. While neohesperidin was highly stable, with *circa* 100% stereomeric excess in all samples, naringin was prone to racemization, especially in mature fruits.

This study also examined the importance of using a sufficient mass of sample to obtain accurate and meaningful measurements, particularly when stereoisomers are concerned.

Keywords: bitter orange; *Citrus aurantium*; flavonoids; stereoisomers; supercritical fluid extraction; supercritical fluid chromatography; two-dimensional chromatography

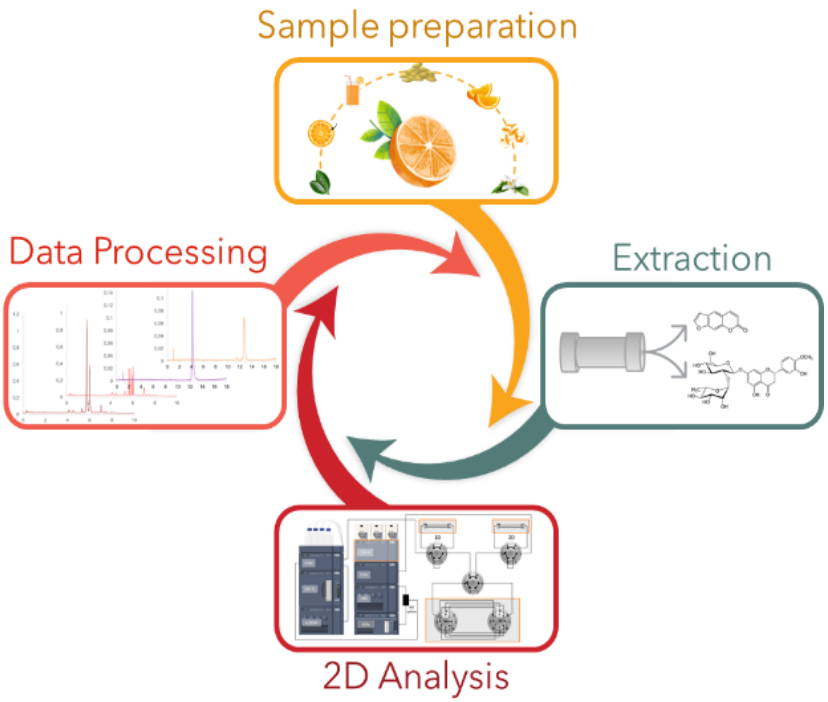

1. Introduction

Flavonoids are phenolic compounds well known for their diverse biological effects such as antioxidant activity (Suntar et al., 2018; Zou et al., 2016), making them promising agents for the prevention and treatment of chronic and neurodegenerative diseases such as Alzheimer's (Abou Baker et al., 2020; Calderaro et al., 2022). In addition to their antioxidant properties, flavonoids have been demonstrated to have anti-inflammatory (Kang et al., 2011; Shen et al., 2017), anti-cancer (Choi et al., 2020; Ren et al., 2003), anti-microbial (Gopal, 2012; Tungmunnithum et al., 2018) and cardiovascular effects (Benavente-García & Castillo, 2008; Testai & Calderone, 2017). Flavonoids are broadly distributed in natural products, including *Citrus aurantium* L. (bitter orange). In addition to being used in culinary preparation as a substitute to lemon juice, or in food supplements (Fugh-Berman & Myers, 2004), where it is supposed to contribute to weight loss, *C. aurantium* is widely used for aromatic and medicinal applications (Maksoud et al., 2021). The bioactivity is mainly related to flavonoids, with naringin and neohesperidin being the most abundant (Castillo et al., 1992). In addition, several of these flavonoids, including the latter two, contain stereocenters in their aglycon root, leading to the presence of stereoisomers (Réset, De Saint Jores, & West, 2024). In the case of aglycon flavonoids, the isomers are enantiomers, while in the case of the glycosylated flavonoids (like naringin and neohesperidin), because the sugar moieties also contain stereocenters, the isomers are diastereomers. Whatever the isomer type, these stereoisomers may differ in their bioavailability and biological activity (Kumar & Pandey, 2013). Consequently, achieving a chiral separation of these flavonoids is important to characterize the bioactivity of individual stereoisomers and to better understand their individual roles in various fields of application (Zhang et al., 2023). For instance, while it is well known that flavonoids are among the main molecules responsible for the bitterness of citrus fruits (Luo et al., 2025), Gaffield *et al*. observed that the 2S isomer of naringin yielded a lower bitterness in grapefruit than the 2R isomer (Gaffield et al., 1975). The determination of enantiomeric (e.e.) or diastereomeric excesses (d.e.) is therefore of interest to compare the distribution of flavonoid stereoisomers in samples from different parts of *C. aurantium* (leaves, peel, pulp, flowers, albedo) and at different stages of maturity (Moulehi et al., 2012).

In recent years, two-dimensional chromatography has become an effective method to separate complex mixtures, especially in natural product analysis (Pirok et al., 2019).

For stereoselective separations, one of the most useful techniques is supercritical fluid chromatography (SFC) (West, 2019). This technique enables rapid separation and analysis of flavonoids using a low-viscosity fluid (supercritical CO_2) as the major component of the mobile phase. SFC uses low volumes of organic solvents, making it a greener analytical alternative to traditional techniques such as liquid chromatography (LC) (West, 2018). When SFC is used in both dimensions of a two-dimensional separation system, it can provide orthogonal separation mechanisms simply through an adequate selection of stationary phases, making it even more powerful. With the addition of mass spectrometry (MS), this setup should be useful to separate isomers that are difficult to distinguish and to reduce problems with overlapping peaks, which are frequent in complex mixtures (Okamoto & Hirata, 2006).

Using the same supercritical CO_2 as major fluid, added with a small portion of ethanol, supercritical fluid extraction (SFE) is ideal for the extraction of low- to medium-polarity flavonoids from naturals products (Atwi-Ghaddar et al., 2023; Herrero et al., 2006). This technique is efficient, selective and environmentally friendly. However, sample preparation is critical to analyte stability and extraction yield. In addition, combining SFE with SFC provides a green approach for the analysis of natural products (Sánchez-Camargo Andrea del Pilar et al., 2016).

In this study, we have examined SFE of the major flavonoids of *C. aurantium* and determined the diastereomeric excesses of naringin and neohesperidin with SFC-SFC-UV-MS analysis in a multiple heart-cutting mode (Réset, De Saint Jores, François, et al., 2024). In this system, the first SFC dimension allowed isolating two target flavonoids from the whole extract, while the second SFC dimension resolved their diastereomers. In particular, sample preparation raised many questions to achieve reliable results. Different organs of the plant were examined (leaves, peel, flowers, albedo and pulp) and at various maturity stages. The main goal was to observe the effects of ripening stages, organ samples, drying procedure and geographical origin of the fruit on the stereoisomeric profile of major flavonoids in this plant.

2. Materials and methods

2.1. Chemicals and samples

HPLC-grade methanol used as the mobile phase co-solvent and sample diluent, ethanol Hipersolv Chromanorm 99.7-100% used as extraction co-solvent, ammonium hydroxide, LC-MS-grade water and formic acid with a purity of 99-100% were

purchased from VWR (Fontenay-sous-Bois, France). CO_2 with a purity of 99.7% was delivered by Air Liquide (Paris, France). Methanesulfonic acid (MSA) and acetonitrile LC-MS grade were purchased from Sigma-Aldrich (Saint-Quentin-Fallavier, France). Ultra-pure water was supplied by a Milli-Q® IQ 7000 system from Merck (Darmstadt, Allemagne). Naringin and neohesperidin standards were acquired from Extrasynthese (Genay, France).

C. aurantium flowers, peels, and leaves were bought from Louis Herboristerie (Charleville-Mézières, France). Fresh *C. aurantium* fruit was purchased from Vergers de Boirie (Menton, France). Other leaves were kindly supplied by Prof. Mohamed Addi from University Mohammed Premier, Oudja, in Morocco.

2.2. Sample preparation and sonication

Fresh *C. aurantium* fruits were manually prepared. Three stages of fruit ripeness were observed: ripe oranges with an orange color, half-ripe oranges with a yellow-orange color and unripe oranges with a green color. For each stage of maturity, the different parts of the orange were separated: peel, albedo, un-seeded pulp, juice and leaves. Samples of albedo, pulp and leaves were freeze-dried. For the peel, one part was placed in the oven and the other in the freeze-dryer. All samples were ground into powder. Since the flowers, skins and leaves from Louis Herboristerie and the leaves from Morocco were supplied as dry material, they were simply ground without further drying.

Samples extracted by sonication were prepared as follows: 1 g of sample was extracted with 15 mL of ethanol (EtOH) or EtOH/H_2O (80/20) for 30 min in an ultrasonic bath. The extract was then centrifuged (20 °C, 8000 rpm) for 5 min and filtered through 0.20 µm, 13-mm diameter PVDF syringe filters from Agilent Technologies (Les Ulis, France) and diluted by 4 in EtOH or EtOH/H_2O 80/20 (depending on extraction conditions) prior to analysis.

2.3. Supercritical fluid extraction (SFE)

2.3.1. Instrumentation

A Nexera UC system from Shimadzu Corporation (Kyoto, Japan) was used for all extractions. The system was composed of a CO_2 pump (LC-30ADsf), a co-solvent pump (LC-30AD) for extraction, and an additional solvent pump (LC-20ADXR) to introduce make-up fluid after the extraction. The instrument included an extractor

(SFE-30A) connected to a Rack Changer II, which housed 48 slots for 5-mL extraction vessels, as well as a back-pressure regulator (BPR) to control pressure within the auto-extractor (SFC-30A). The extraction system was directly linked to a fraction collector (FRC-40SF). Instrument control was managed using LabSolutions LC-MS version 5.120 from Shimadzu Corporation.

2.3.2. SFE conditions

Samples were introduced in 5-mL stainless steel extraction vessels. The sample weight varied between 50 mg and 1 g, mixed with dispersant (diatomaceous earth). A cellulose filter was placed at the bottom of the vessel, and cotton was placed at the top, respectively to filter the extract and fill the cell entirely.

Based on previous works that examined SFE of flavonoids (Atwi-Ghaddar et al., 2023), the co-solvent used was a mixture of ethanol and water, as further described below. A constant flow rate of 3 mL/min was used. A make-up flow rate of EtOH/H_2O 80/20 was set at 0.7 mL/min to avoid sample precipitation after CO_2 depressurization at the BPR outlet.

The fractions recovered from SFE were evaporated to dryness under a nitrogen flow, then resolubilized in 4 mL of 80/20 EtOH/H_2O and filtered through 0.20 µm, 13-mm diameter PVDF syringe filters.

2.3.3. SFE Design of experiment (DoE)

To optimize the SFE conditions, a DoE was developed. A Box-Behnken design (BBD) was previously described for the extraction of polar flavanol molecules from a different plant (Atwi-Ghaddar et al., 2023). The same design was reproduced here to extract glycosylated flavanones. The three factors used in this study were:

- temperature (T), varying from 40 to 80 °C,
- total co-solvent (ethanol-water) percentage (C), varying from 10 to 30% in pressurized CO_2,
- water percentage added to ethanol (W), varying from 0 to 20%,

with three levels coded as (+1) for the highest, (0) for the middle point and (-1) for the lowest level (Table S1). Two responses were considered: peak areas measured in the first-dimension SFC analysis for the two target compounds (naringin and neohesperidin) and the corresponding mass of flavonoids extracted, determined from calibration curves constructed with standard compounds (Réset, De Saint Jores,

François, et al., 2024). A total of 17 experiments were carried out in a random fashion, including 5 replicates at the central point (see supplementary information, Table S2 and Figure S1). 50 mg of bitter orange dry flower sample were used for each experiment in this design.

Data reprocessing, model calculation and graph visualization were performed with the XLSTAT 19.03 software (Addinsoft, Paris, France).

2.4. SFC-MS analysis

2.4.1. Instrumentation

The supercritical fluid chromatography system was based on a Waters Corporation (Millford, MA, USA) ACQUITY Ultra Performance Convergence Chromatography™ (UPC²®). It was equipped with an autosampler with a partial loop volume injection system, an automated back-pressure regulator (BPR), a 2-columns oven compatible with 150 mm-length columns, via column switching valves. The system also included a binary solvent delivery pump compatible with a maximum mobile phase flow-rate of 4 mL/min and a maximum pressure of 414 bar. Two detectors were available: a diode-array detector (ACQUITY PDA®) and a single-quadrupole mass spectrometer (MS) with an electrospray ionization (ESI) source (ACQUITY QDa®). An isocratic solvent manager was used as a make-up pump and was positioned after the diode-array detector and before a flow splitter, where one portion was sent to the BPR and the other to the MS. The use of MSA in the mobile phase involved adapting the exhaust valve of the QDa instrument, as MSA may cause corrosion on certain parts.

The instrument was modified in-house to achieve a multiple-heart-cut SFC-SFC configuration, with the addition of three 2-position 6-port valves and loading loops, as previously described (Réset, De Saint Jores, François, et al., 2024).

Empower® 3 was used for chromatographic acquisition and for data treatment.

2.4.2. Chromatographic conditions

Two different columns were used. The first-dimension (dim1) column was ACQUITY UPC² Torus DEA (100 × 3.0 mm, 1.7 µm) from Waters, preceded with a Torus DEA pre-column (5.0 × 2.1 mm). This served to resolve naringin and neohesperidin from the sample and collect them individually for further analysis in the second dimension. The second-dimension (dim2) column was CHIRALPAK IB-3 (150 × 4.6 mm, 3.0 µm) from Chiral Technologies (Illkirch-Graffenstaden, France). This served to separate the

diastereoisomers of naringin on the one hand, neohesperidin on the other hand. Thus, diastereomeric excesses (d.e.) could be measured.

The mobile phase used was CO_2 with MeOH containing 0.1% MSA. The injection volume was 5 µL. The gradient programs, including variation of solvent composition, back-pressure and flow-rate, are presented in Table S3.

The column oven was heated to 30 °C and the sample compartment was kept at 10 °C. All chromatograms were recorded in the 210-400 nm range, with 1.2 nm resolution. Scan rate was 20 Hz. Visualization and peak integration in UV were done at 280 nm for standards and sample.

The SFC dim1 method used was previously developed by Molineau *et al.* to separate a large number of flavonoids, including regio-isomers (Molineau et al., 2020). The SFC dim2 method was optimized to resolve glycosylated flavonoid diastereoisomers. As a result, combining the two methods, the risk of co-elution of isomeric species after two complementary methods should be minimal.

2.4.3. Mass spectrometry conditions

The optimal ESI-MS parameters were as follows: make-up fluid was either MeOH (section 3.4), or MeOH comprising 20 mmol.L^{-1} NH_4OH and 2% H_2O (section 3.2, 3.3), pumped at 0.4 mL/min; probe temperature 600 °C; ion source temperature 120 °C; cone voltage 10 V; capillary voltage +/- 0.3 kV; scan rate 3.7 Hz. The mass range for total ion recording was set from *m/z* 100 to 1000. The *m/z* values followed in single-ion monitoring (SIM) were: *m/z* 303 and *m/z* 273 corresponding to the aglycone protonated ion $[M - C_{12}H_{22}O_9 + H]^+$ for the positive mode, *m/z* 705 and *m/z* 675 corresponding to the MSA adduct $[M + MSA]^-$ for the negative mode. Negative mode was used for processing SFC-SFC-MS data.

Diastereomers may have different ionization efficiency. However, we had previously verified that the d.e. values obtained by UV and MS on neohesperidin and naringin standards were identical. Therefore, either one or the other detector could be used. However, since co-elution of non-isobaric compounds was observed in real samples of *C. aurantium*, UV was inadequate in this case and the MS data was retained for the calculations of d.e. values. Only for the reprocessing of the other cases, when no co-elution was observed, the UV data was examined.

2.5. LC-MS analyses

LC-MS analyses were performed on an Ultimate 3000 RSLC system, coupled with a TSQ Endura triple quadrupole mass spectrometer (Thermo Fisher Scientific Inc., Waltham, MA), equipped with an electrospray ionization source (H-ESI). The column was SymmetryShield RP18 (150 x 3 mm, 3.5 µm) from Waters. A binary solvent system was used as mobile phase, solvent A consisting of water with 0.1% (v/v) formic acid and solvent B consisting of acetonitrile with 0.1% (v/v) formic acid. The flow rate was 0.5 mL/min, with a gradient elution where solvent B was increased from 5% to 100% in 5 min. The optimal MS parameters were as follows: spray voltage 3500 V in positive mode, 3200 V in negative mode; ion transfer tube temperature 356 °C; vaporizer temperature 420 °C; scan range *m/z* 100-1000; scan rate 1000 Da/sec. For product ion scan: collision gas pressure 1.5 mTorr; collision energy 30 V for the negative mode, 15 V for the positive mode.

3. Results and discussion

3.1. SFE conditions optimization

To optimize SFE conditions, a DoE was conducted on dry flowers petals. This sample was available in large quantities (larger than many of the other parts), making it ideal for the DoE. The three parameters varied and their levels are presented in Table S1.

Firstly, from the examination of samples, it soon appeared that high temperatures (60 and 80 °C) were inappropriate for these samples, since they resulted in a brown and viscous extract, probably containing burnt sugars, which tended to clog the system. Although temperature may be a significant parameter in the extraction of flavonoids in different samples, this caramel-like extract was inadequate for further redissolution and analysis. Note that previous samples examined in comparable conditions had not necessarily shown any such issue.

Secondly, from the observation of DoE responses (peak areas of the target flavonoids and total mass of the extract), it appeared that experimental variability was high, with relative standard deviation at the central point reaching about 50% in terms of peak area variability, and about 30% for the total mass of flavonoids extracted. This high variability may be partly due to the SFE process, where significant variability is often observed, but may have been aggravated here by the reduced amount of sample used (50 mg). Another hypothesis may have been related to sample degradation during the experiments, but this can be easily ruled out, as no regular decrease was observed

among the five central point replicates that were spaced out in the DoE experiments, rather a random variation.

However, as the total variance was still much larger than the variance at central point (over 100% for the peak areas and about 70% for the total mass of flavonoids extracted), the results were still amenable to interpretation.

Different models were examined to fit the data, considering linear and non-linear models, with or without interaction terms. In all cases, temperature was observed to be non-significant, possibly related to the above-described difficulties. The best fits were obtained with quadratic models, with only significant terms being reported (see Figure S2 for further details on the models). The model obtained for the extracted mass is presented in Eq. (1):

$$\text{Extract. mass} = 11.80 + 5.18 \times C + 7.46 \times W - 2.68 \times C^2 + 2.65 \times W^2 + 6.50 \times C \times W \quad (1)$$

With n = 17; R^2 = 0.823; RMCE = 4.165.

From the models obtained and the observation of response curves, it appears that maximum extraction was obtained with the largest overall proportion of co-solvent (30% in CO_2), comprising the largest proportion of water (20% in ethanol). This is further illustrated in Figure S3, representing the response curves depending on co-solvent proportion and water proportion. Note that the optimum point may be situated outside the design space, but we were unwilling to further increase the proportion of co-solvent, or the method would lose its ecological advantage. As observed above, low temperature should be preferred to avoid burning sugars, especially as other plant organs to be evaluated later were suspected to contain much more of them. Consequently, the extraction conditions retained for further experiments were: 40 °C, with 30% co-solvent comprising ethanol and water in 80/20 proportions.

Three experiments were repeated in these conditions. The variance observed was lower than observed at the central point (relative standard deviation was about 10%), suggesting that the larger temperature (60 °C) may have contributed to the experimental variability at the center of the experimental domain. However, further experiments with different organs of the plant still showed significant variability so other causes of variance had to be examined.

3.2. Examination of sample mass

As mentioned above, SFE extraction conditions were optimized for dried flowers sample with a constant mass of 50 mg. However, a high variability was obtained for the central point replicates, and was further observed in the conditions of maximum extraction for other plant organs, prompting further examination of the best sample mass to introduce for accurate measurements. For this purpose, extractions were performed using increasing quantities of orange peel (PeDS), ranging from 25 mg to 1 g. Two independent samples (sample 1 and sample 2) were prepared and analyzed for each mass level. The extracts were all analyzed with the SFC-SFC-DAD-MS method, where the first dimension served to measure the quantity of naringin and neohesperidin in the extract, then, after loading them in storage loops, the second dimension provided a stereoisomeric separation for each of them to measure diastereomeric excess (d.e.).

First, it was important to determine whether the sample mass introduced in the extraction vessel had an impact on the extraction yield. Indeed, when large quantities are used and solubility of the target analytes in the extraction fluid is low, the quantity extracted may not be proportional to the quantity introduced in the extraction vessel. For this purpose, the UV peak areas observed in the first-dimension separation were measured. From the extracts, two distinct solutions were prepared: constant volume (blue) and constant concentration (green) (Figure 1).

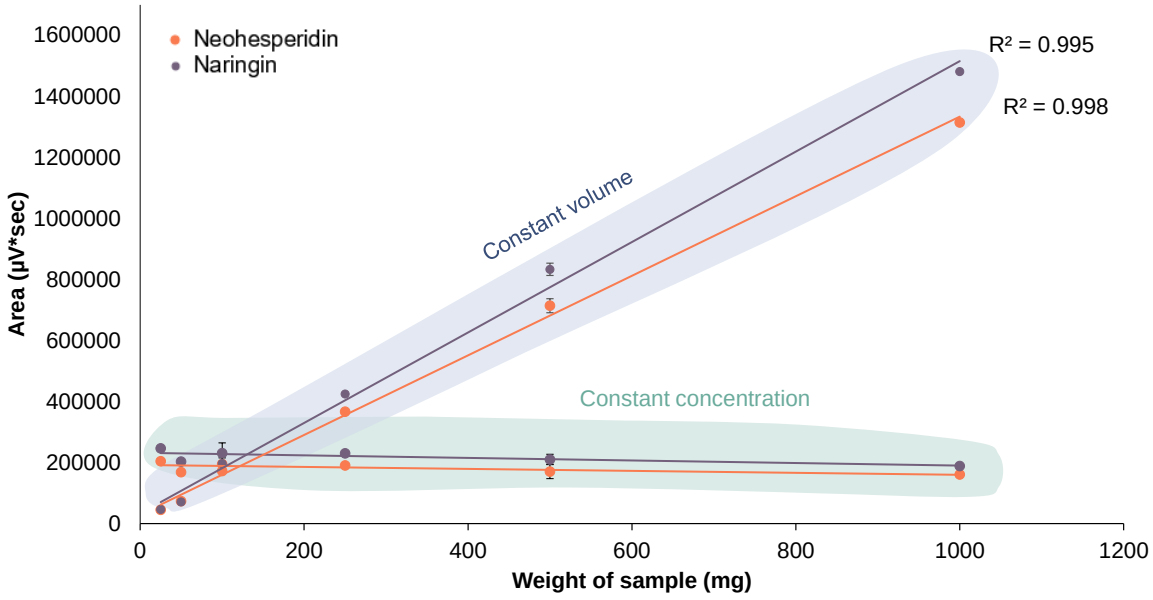

Figure 1 – Peak areas obtained from neohesperidin and naringin during the 1D analysis of a bitter orange peel sample (PeDS) extracted by SFE on the first SFC analysis dimension (dim1). Analysis with samples taken at constant volume (blue) and analysis at constant concentration (1 mg/mL).
Analysis conditions for dim1: ACQUITY UPC² Torus DEA (100 × 3.0 mm, 1.7 µm), co-solvent: MeOH + 0.1% MSA, 150-110 bar, 1.7-0.6 mL/min (gradient conditions in Table 1, gradient a)

In the “constant volume” configuration, each extract was redissolved in an identical volume of dissolution solvent, so that the concentration increased proportionally to the mass introduced. The results showed a linear increase in peak area with sample mass for both compounds analyzed. This relationship was characterized by high determination coefficients (R^2 = 0.998 for neohesperidin and R^2 = 0.995 for naringin), confirming an excellent correlation between the mass of sample introduced in the extractor and the amount of flavonoids extracted. This also indicates that the solubility limit was not reached during these experiments.

In the “constant concentration” configuration, the dissolution volume was adjusted depending on the mass of extract, in order to obtain identical concentration in all vials. As observed in Figure 1, the measured peak areas remained relatively stable despite the increase in bulk mass. This approach allowed samples to be compared on an equivalent basis, regardless of their mass. With this method, it appeared that the extraction yield was stable, allowing to conclude that the experiments conducted at different sample masses were comparable.

In addition to the extraction yield, a significant response to consider at this stage was the diastereomeric excess (d.e.) measured for the two target flavonoids. Indeed, diastereoisomers may have different solubility in the extracting fluid, and they may thus have been differently impacted by the sample mass. The results are shown in Figure 2, in the form of histograms comparing the d.e. (%) of neohesperidin (Figure 2A) and naringin (Figure 2B) for each mass level and for the two samples extracted individually. For both target compounds, it appears that the results were not repeatable when the sample amount was lower than 250 mg for neohesperidin and 500 mg for naringin. At low sample masses (from 25 to 100 or 250 mg), a large difference in d.e. was observed between the two samples. Note that the system was thoroughly rinsed between two samples, therefore we cannot suspect any carry-over effect. The increase in d.e. with extracted mass suggested that a minimum threshold was required to obtain a reliable

representation of the stereoisomers. For neohesperidin, a high d.e. (above 90%) was observed in repeatable conditions. For naringin, the d.e. was lower, reaching 40% in repeatable conditions.

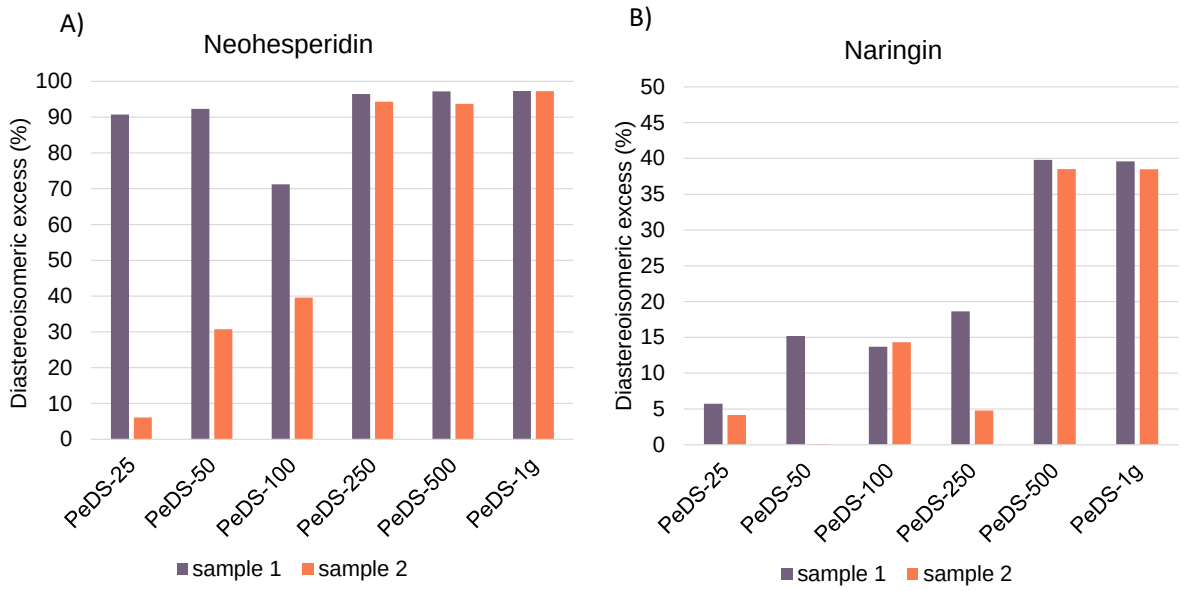

Figure 2 – Diastereomeric excess of Neohesperidin and naringin measured in SFC-SFC analysis of a bitter orange peel sample (PeDS) at different mass levels (25 mg to 1 g). Analyses performed in duplicate (sample 1 and sample 2).
Analysis conditions for dim1 were identical to Figure 1. Analysis conditions for dim2: CHIRALPAK IB-3 (150 × 4.6 mm, 3.0 µm), co-solvent: MeOH + 0.1% MSA (gradient conditions in Table 1, gradient b), 150 bar, 2.0 mL/min.

Thanks to the observations in Figure 1, we may conclude that the variations observed in the d.e. values (Figure 2) were not due to a difference in extraction efficiency (related to analyte solubility), but rather to secondary analytical effects (matrix effect, detection bias, or different isomer proportions in small samples). However, the use of 1 g of sample in SFE proved technically problematic, leading to recurrent clogging of the system. For this reason, a compromise had to be found between analytical reproducibility and technical feasibility. For subsequent experiments, it was determined that low sample masses (100-200 mg) were acceptable when d.e. values were not measured and only the extraction yield was of interest, while a minimal 500 mg mass should be used to determine d.e. values.

3.3. Analyte stability

To further investigate variability in lower extracted masses, stability studies were carried out on a sample of bitter orange peel.

3.3.1. Possibility of conversion

In the second-dimension SFC-UV chromatogram obtained for a peel sample, partial co-elution was observed in the retention windows corresponding to the neohesperidin diastereomers and the naringin diastereoisomers. Mass spectrometry was used to determine the identity of the coeluted peaks, and suggested that these co-eluting species would correspond to brutieridin and melitidin, respectively (Figure 3). These two compounds are structurally close to neohesperidin and naringin, as they share the same aglycon root and the same sugar moiety, but have an additional 3-hydroxy-3-methyl-5-oxopentanoate group grafted onto the disaccharide skeleton via an ester function. Due to its possible lability, this bond could be hydrolyzed in acidic media during SFE extraction or SFC analysis and be a cause for peak area variability. Indeed, the combination of CO_2 and short-chain alcohols like methanol and ethanol produces a somewhat acidic environment through the formation of alkoxylcarbonic acid (West et al., 2017). In addition, the extraction conditions included water, further acidifying the medium with the formation of carbonic acid, while the analysis conditions included methanesulfonic acid, which is a strong acid. Thus, conversion of brutieridin to neohesperidin and conversion of melitidin to naringin could occur either during the extraction, or during the analysis.

First, two orange peel extracts (200 mg) prepared by SFE on the one hand and sonication on the other hand were subjected to LC-MS analysis in order to evaluate the possible contribution of extraction conditions on analyte degradation. The aim was to detect any conversion of brutieridin to neohesperidin, resulting from a break in the ester group. The $[M-H]^-$ deprotonated molecular ions were followed with single-ion monitoring, with values of *m/z* 609 for neohesperidin and *m/z* 753 for brutieridin. The areas of the corresponding peaks were measured (Table 1), and the intensity ratios calculated. The results show that the ratios were comparable between the two extraction methods, indicating that the SFE step did not cause any significant degradation of brutieridin to neohesperidin.

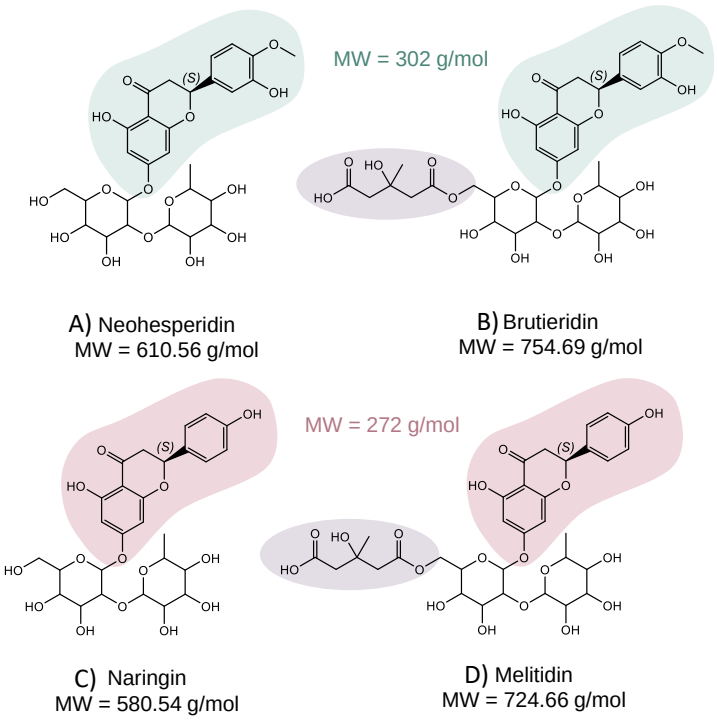

Figure 3 – structures of the major isomers: Neohesperidin (A), Brutieridin (B), Naringin (C) and Melitidin (D)

Table 1 – Peak areas and ratios obtained for neohesperidin (m/z 609) and brutieridin (m/z 753) with LC-MS analysis of two samples of bitter orange peel (Pe-DS) extracted with maceration or SFE. Analysis conditions: SymmetryShield RP18 (150 x 3 mm, 3.5 µm). solvent A: H_2O + 0.1% FA, solvent B: ACN + 0.1 % FA, gradient: 5% to 100% of B in 5 min, 0.5 mL/min, ion source: ESI.

		Area (µV*sec)	
		Maceration	SFE
1	Neohesperidin (m/z 609)	211166108	192656524
2	Brutieridin (m/z 753)	179542576	177697634
	Ratio (1/2)	1.18	1.08

The next step was to assess the potential impact of the acidic SFC conditions on brutieridin stability. For that, a peel extract obtained by SFE was analyzed in triplicate using the gradient method (Table S3) in SFC-SFC-MS. The brutieridin/neohesperidin peak area ratios were calculated for each analysis (Table 2). Although these ratios were higher than those observed in LC-MS, it was not possible to conclude on the impact of SFC conditions, as the ionization sources used for the two analyses were not identical, and the fluid composition entering the ionization source was different between LC-MS and SFC-MS experiments. Hence the ionization yield of the two analytes may have been different between the two conditions. However, the repeatability of the ratios between replicates suggested that, even if there was some conversion of brutieridin to neohesperidin during the SFC analysis, this remained constant and controlled.

Table 2 – Peak areas and ratios obtained for neohesperidin (m/z 609) and brutieridin (m/z 753) with three replicate SFC-SFC-MS analyses of a sample of bitter orange peel (Pe-DS) extracted with SFE. Analysis conditions for dim1: ACQUITY UPC² Torus DEA (100 × 3.0 mm, 1.7 µm), co-solvent: MeOH + 0.1% MSA, 150-110 bar, 1.7-0.6 mL/min (gradient conditions in Table S3, gradient a). Analysis conditions for dim2: CHIRALPAK IB-3 (150 × 4.6 mm, 3.0 µm), co-solvent: MeOH + 0.1% MSA (gradient conditions in Table S3, gradient b), 150 bar, 2.0 mL/min.

		Area (µV*sec)		
		Rep 1	Rep 2	Rep 3
1	Neohesperidin (m/z 609)	39865346	29219825	27316053
2	Brutieridin (m/z 753)	13125267	9459259	6875987
	Ratio (1/2)	3.04	3.09	3.97

3.3.2. Stability in solution

When samples were analyzed with the SFC-SFC-UV system in a multiple heart-cut configuration, the compounds of interest were temporarily stored in transfer loops before being transferred to the second dimension. This delay, which could last several

hours when several fractions were stored for second-dimension analysis, could be a critical factor in terms of sample stability. Furthermore, although extraction replicates were prepared back-to-back, only the first one to be dried down was injected immediately. Subsequent samples remained in the cooled (10°C) automated injector rack, sometimes for one or more days, before being analyzed. It was therefore essential to determine the stability window of the samples, in order to assess any degradation and adjust the preparation and storage conditions as best as possible.

For this stability study (Figure S4), a sample of orange peel was extracted by SFE, then solubilized in an ethanol/water mixture (80/20, v/v), and analyzed repeatedly over a period of six days. To validate the results, a mixture of neohesperidin and naringin standards was subjected to the same conditions and process. During the whole stability study, the samples and standards were simply stored in the automated injector rack at 10 °C.

The results showed that after six days, no degradation was observed for either the peel sample or the standards. In the peel sample, the d.e. values of neohesperidin were stable at 100%, indicating that only one diastereomer was observed. On the other hand, some fluctuations of around 5% were observed for naringin. However, these variations do not follow a trend, suggesting that they are not the result of sample degradation, but probably of analytical variability. This is probable since the excess is small, the composition of naringin diastereoisomers being close to 50/50.

3.4. Determination of diastereomeric excess in *C. aurantium* samples

Having thoroughly examined the extraction conditions and stability of the stereoisomers, we were confident that the SFE and SFC-SFC-MS methods provided reliable results, and could then proceed to examine a variety of samples.

3.4.1. Fruit parts

In this section, three stages of fruit maturity were studied: ripe, half-ripe and unripe. For each of these maturity stages, different parts of the fruit were extracted: peel, albedo and pulp, then analyzed with SFC-SFC-MS to determine the d.e. values of neohesperidin and naringin.

In the case of neohesperidin, whatever the stage of ripeness, the d.e. remained very high, between 98% and 100% for all three parts of the orange. In other words,

neohesperidin showed very high stereochemical stability (Figure 4A), with one diastereoisomer being largely dominant. The lack of variability may mean that neohesperidin biosynthesis is little affected by developmental or environmental processes such as UV exposure. This suggests that the downstream enzymes involved in its biosynthesis (such as flavanone 3-hydroxylase or other glycosyltransferases (Ku et al., 2020; Ma et al., 2023)) maintain high stereochemical selectivity, independently of maturity, and/or that neohesperidin and its aglycon precursor hesperitin are both rather stable and unaffected by other non-enzymatic ring-opening reactions (Figure 5).

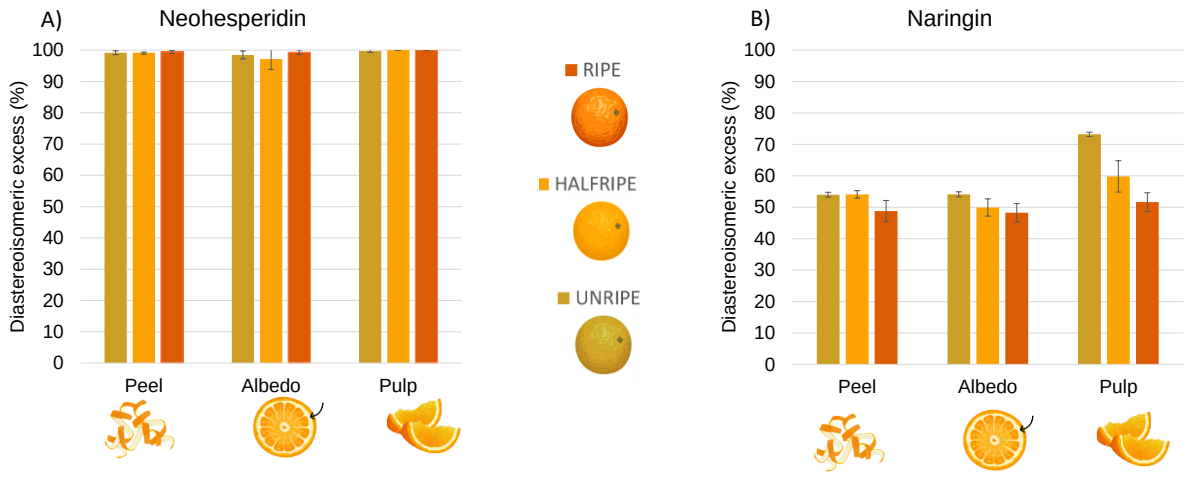

Figure 4 – Comparison of the d.e. of neohesperidin (A) and naringin (B) for 3 maturity stages (unripe, half-ripe and ripe) and for 3 parts of the fruit (peel, albedo and pulp). Error bars are based on two replicates. SFC-SFC conditions are identical to Figure 2.

On the other hand, the d.e. values observed for naringin were lower (Figure 4B), in the 45 to 75 range, thus indicating that both diastereomers were present with a significant concentration. In addition, some variation was observed with the stage of maturity, with bigger variations observed for the pulp samples, showing a decrease of about 70% to 50% between the unripe and ripe stages, indicating progressive racemization of naringin. To understand the differences between naringin and neohesperidin and the variations with maturity, the enzymatic and non-enzymatic pathways must be better explained. They are detailed in Figure 5.

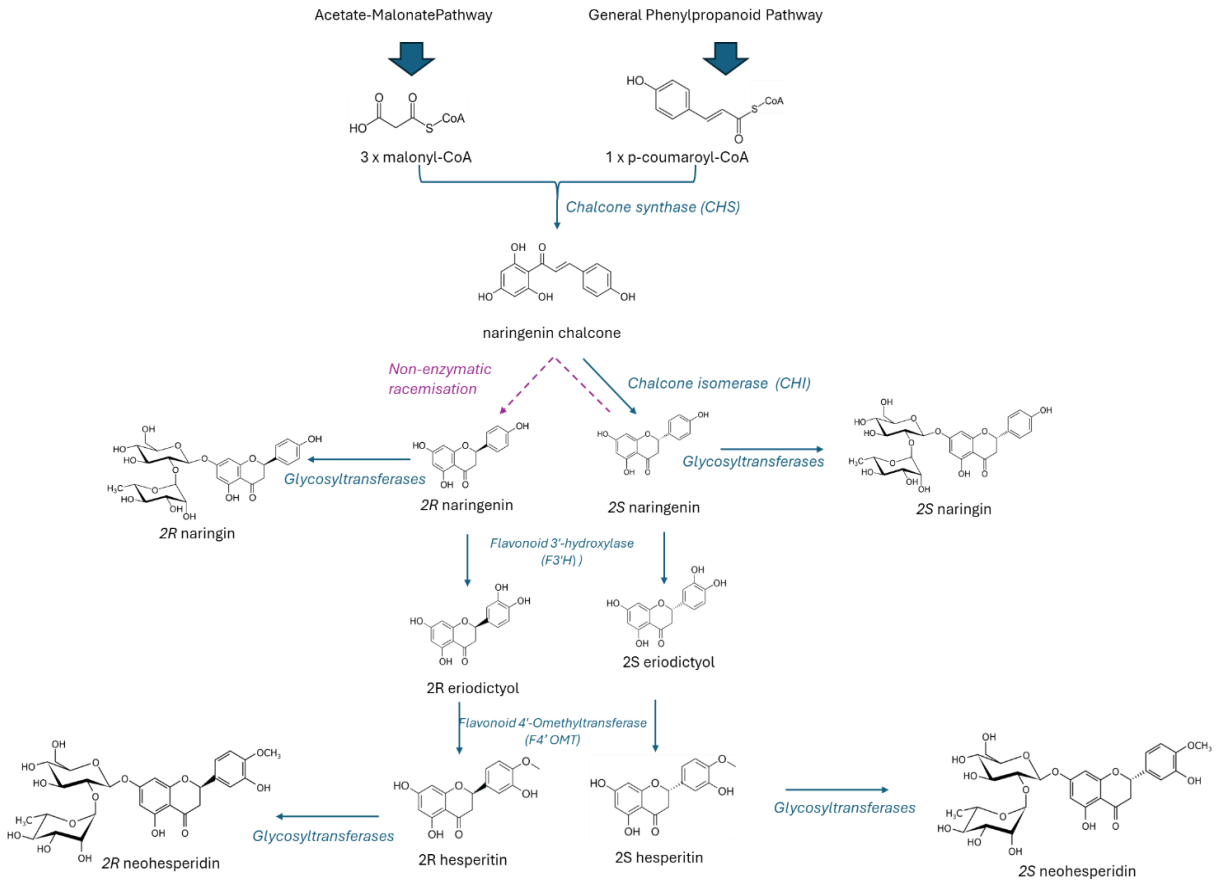

Figure 5 – Biosynthesis of 2R-2S-neohesperindin and 2R-2S-naringin

First, starting from a chalcone precursor, the chalcone isomerase (CHI) catalyzes the stereospecific cyclization into the sole 2S-naringenin isomer, the aglycone form of naringin (Ni et al., 2020). The 2S enantiomer of hesperitin, the aglycon form of neohesperidin, is subsequently formed from the 2S-enantiomer of naringenin, through the action of downstream enzymes: flavonoid 3'-hydroxylase (F3'H), flavonoid 4′-O-methyltransferase (F4'OMT) and further glycosyltransferases.

Furthermore, the 2S-naringenin enantiomer may also face ring-opening and non-stereospecific closing of the cycle through non-enzymatic processes (Caccamese & Chillemi, 2010), thereby causing progressive racemization through the formation of both R and S enantiomers (see "non-enzymatic racemization" pathway in Figure 5). This may be favored by UV exposure and high temperature (Wistuba et al., 2006). Finally, the 2R-enantiomer of naringenin may also yield a parallel cascade to produce 2R-naringin, 2R-hesperitin and 2R-neohesperidin.

The CHI enzyme-catalyzed step has been estimated to be 107 times faster than spontaneous cyclization (Bednar & Hadcock, 1988). This supports the initial formation

of 2S enantiomers with a large enantiomeric excess. Thus, in the absence of further metabolism, the accumulation of the S-isomer of naringin is thermodynamically favored by enzymatic production, while the R-isomer will be formed over time by the non-enzymatic and non-stereospecific racemization as described above. The gradual racemization of naringin with increasing maturity observed in the present study is consistent with previous literature related to the maturation of citrus fruits (Caccamese et al., 2003; Caccamese & Chillemi, 2010; Gaffield et al., 1975), in particular in pummelo and sour oranges (Caccamese et al., 2007; Caccamese & Chillemi, 2010).

Since the enzymes downstream CHI to produce subsequent intermediates do not exhibit as strict a stereochemical preference as CHI, the stereochemistry of these intermediates therefore depends on the efficiency (substrate binding and turnover) of the subsequent steps, in particular the following F3'H step. The S-isomer versions of the subsequent intermediates therefore result from the use of the S-naringenin precursor having been formed both non-enzymatically during the racemization step as well as by stereospecific enzymatic production from CHI (the latter being favored from a thermodynamic point of view), while the R-intermediates are formed after conversion of the R-naringenin produced solely by non-enzymatic formation.

In our case, we can assume that the relative concentrations of R- vs. S-naringenin across plant organs and maturation stages will depend on the binding affinity and catalytic turnover of F3'H toward the R- and S- isomers, as well as the thermodynamic reaction equilibrium of this enzymatic step at cellular level in these different plant organs. A low conversion rate of F3'H from S-naringenin formed by CHI allows for a higher formation of R-naringenin, and other subsequent R-intermediates, such as the here studied hesperidin, by giving more time to the non-enzymatic racemization reaction to occur. It is noteworthy that in the case of hesperitin, binding affinity and catalytic turnover of F3'H to S-naringenin formed by CHI will favor the accumulation of S-hesperitin by limiting the slower non-enzymatic racemization reaction.

In other words, the fact that neohesperidin retains a high d.e. value in all samples and conditions (Figure 4A) suggests the sole use of the 2S isomer of naringenin for the downstream biosynthetic steps, leading to the accumulation of 2S-neohesperidin.

Moreover, it is worth mentioning the d.e. may also be influenced by the possibility of physical interactions between enzymes. Indeed, CHI together with other enzymatic partners involved in flavonoid biosynthesis have been shown to form a metabolon (Burbulis & Winkel-Shirley, 1999), a multi-enzyme complex in which soluble enzymes,

including CHI, are anchored to the endoplasmic reticulum by association with membrane enzymes belonging to the cytochrome P450 (CYP) family such as F3'H, which serve as a stabilizing platform for this supramolecular enzymatic complex, allowing rapid channeling of intermediates between active sites, increasing local concentrations and preventing the formation of side-products. Thus, in our case, the possible existence of such metabolon could favor the accumulation of S-hesperidin and so the depletion of S-naringenin.

Finally, to explain the differences between the fruit organs, another option is that the naringin diastereomers have differential mobility in the fruit, resulting in varying stereoisomeric compositions when a single part of the fruit is observed. As the pulp contains a liquid portion (or juice), the analyte mobility may be higher there than in dryer tissues like albedo and peel.

3.4.2. Diastereomeric excess of other plant organs

After characterizing the d.e. of neohesperidin and naringin in the different fruit fractions (peel, albedo and pulp), the analysis was extended to other vegetative organs (leaves and flowers) and to compare samples from various geographical origins.

3.4.2.1. Leaves of different geographical origins

Three leaves samples were compared (Figure 6A): fresh leaves from the harvest of oranges at Vergers de Boirie and that were dried in-house, leaves bought as dried material from Louis Herboristerie, and leaves received as dried material from Oujda in Morocco.

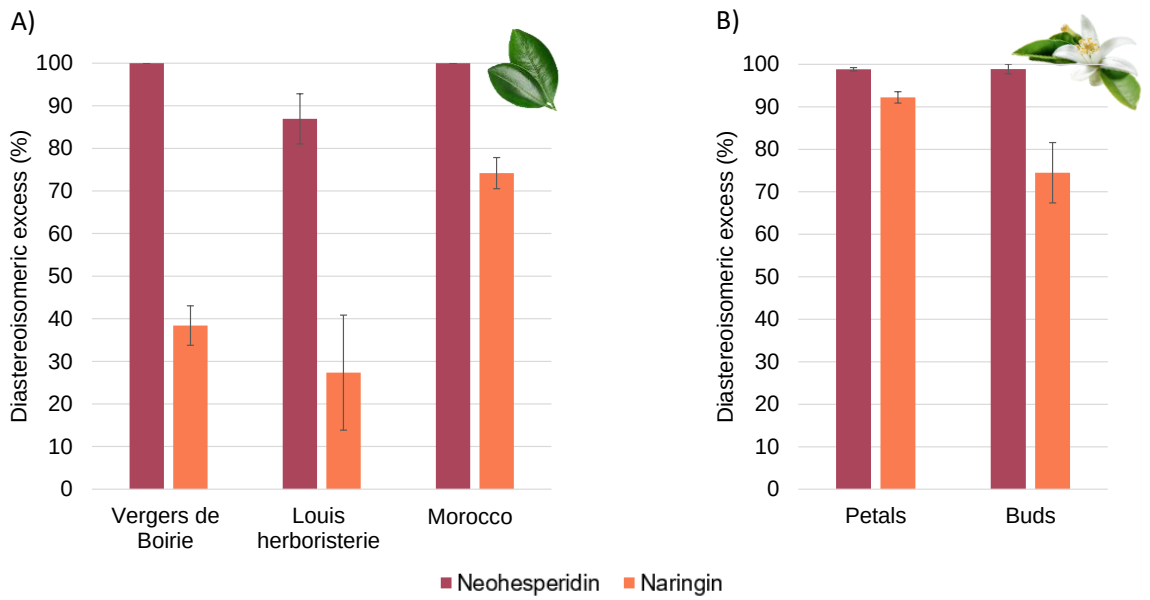

Figure 6 – Comparison of the d.e. values of neohesperidin (purple) and naringin (orange) for two plant organs: leaves (A) and flowers (B). The leaves come from different sources (Vergers de Boirie, Louis herboristerie and Oudja in Morocco). Error bars are based on two replicates. SFC-SFC analysis conditions are identical to Figure 2.

In Figure 6A, neohesperidin showed a high d.e. comprised between 85 and 98% in the three samples, confirming its stability already observed in fruit tissues, which showed its resistance to variations related to the environment or post-harvest treatments. In contrast, naringin showed marked variations depending on the origin. Moroccan leaves showed a high d.e. (around 75%), close to that observed in fresh orange pulp and peel. The d.e. values were lower (around 40%) for the leaves from Vergers de Boirie and even lower (around 30%) for the leaves of Louis Herboristerie, accompanied by greater inter-sample variability.

These differences could reflect less controlled drying or storage conditions, greater exposure to UV light, or pre- or post-harvest degradation. Furthermore, commercial samples did not come from the same harvest, thus climatic or agronomic variations may also have impacted the results.

3.4.2.2. Flowers: comparison between petals and flower buds

Two types of tissue were studied: flower petals and flower buds (Figure 6B), both provided by Louis Herboristerie. As with the previous samples, the d.e. of neohesperidin was greater than 95%, once again demonstrating its stability whatever

the nature of the plant tissue. For naringin, the d.e. was also high in petals (around 90%), but lower in buds (around 70%), with larger variability.

3.4.3. Influence of drying method on orange peels

Following the observations on dry leaves, the influence of drying method on flavonoid d.e. values may be questioned. Two drying methods were applied on the peels of ripe oranges harvested at Vergers de Boirie. The first method was based on freeze-drying, a cold vacuum dehydration process, while the second was a conventional oven drying. The samples obtained in this way were compared with a commercial sample from Louis Herboristerie, delivered as dry material, and for which the post-harvest treatment conditions (drying, storage, exposure to light) were not known. The results are presented in Figure S5.

Neohesperidin had a very high and constant d.e. close to 100% in all three types of samples. This stability suggests that this molecule is not very sensitive to drying conditions or heat treatments, which indicates strong resistance to isomerization.

On the other hand, naringin always showed a significantly lower d.e. than neohesperidin. Although the freeze-dried and oven-dried samples showed comparable values of around 50%, the commercial sample showed a significantly lower d.e. (around 30%). This decrease in d.e. could be explained by increased exposure to degrading factors such as light (particularly UV), humidity, unsuitable temperatures or possible metabolization by associated bacteria such as Actinobacteria, known to be able to act on naringenin derivatives (Martín & Liras, 2022), during the drying or storage stages, which favored isomerization or partial degradation of naringin. It should also be noted that the samples from Louis Herboristerie did not come from the same harvest as the other peels tested. Consequently, variables such as geographical location (edaphic and climatic variations) and agronomic practices could also have influenced the stereochemistry of the compounds analyzed.

Thus, although the drying method seemed to have little influence on the stereochemistry of neohesperidin, naringin appeared to be more vulnerable, particularly under post-harvest conditions. These observations underline the importance of controlling the processing methods used to preserve the flavonoids of interest.

4. Conclusion

This study showed that SFE extraction from low sample masses results in consistent results in terms of overall extraction yield, indicating consistent extraction efficiency, but high variability in the ratios of stereoisomers, probably resulting from local variability in the different matrices examined. To achieve a reliable measurement of stereoisomeric ratio, a minimum sample mass of 500 mg was required to achieve a good balance between analytical reproducibility and technical constraints. In addition, it was demonstrated that the extraction conditions did not significantly degrade the flavonoid compounds examined. The impact of acidic analysis conditions could not be ascertained but appeared to be repeatable.

The various plant parts studied showed that neohesperidin was particularly stable and unaffected by UV, enzymatic or non-enzymatic reactions, or fruit ripening, as the major diastereoisomer was present in all conditions, with d.e. values nearing 100%. Naringin, on the other hand, appeared more sensitive to these effects, with varying stereoisomeric ratios observed among the samples, ranging from 30 to 90%.

These variations can affect the taste, bioavailability, and biological characteristics of flavonoids. Finally, it is important to regulate cultivation and processing conditions to maintain flavonoid stereochemistry in plant matrices, especially when application for therapeutic purposes is desired.

Acknowledgments

Région Centre Val-de-Loire is acknowledged for a PhD grant allocated to Laurine Réset. Shimadzu Corporation is acknowledged for the Nexera UC system let at our disposal. Prof. Mohamed Addi from University Mohammed Premier, Oudja, in Morocco is acknowledged for providing dry leaves. ICOA is supported by the University of Orleans, the National Centre for Scientific Research (CNRS), the projects CHemBio (FEDER-FSE 2014-2020-EX003677), Valbiocosm (FEDER-FSE 2014-2020-EX003202), Techsab (FEDER-FSE 2014-2020-EX011313), QUALICHIM (APR-IA-PF 2021-00149467), ESTIM-ICOA (CPER / FEDER-FSE+ 2021-2027-00022860), the RTR Motivhealth (2019-00131403) and the Labex programs SynOrg (ANR-11-LABX-0029) and IRON (ANR-11-LABX-0018-01). We also thank the SALSA platform for LC-MS analyses.

CRediT author statement

Laurine Réset: Conceptualization, Methodology, Validation, Formal analysis, Investigation, Writing – Original Draft, Vizualization

Bibi Ousseni: Investigation, Validation

Laëtitia Fougère: Investigation

Christophe Hano: Writing – Review & Editing, Vizualization

Clément De Saint Jores: Conceptualization, Methodology, Writing – Review & Editing, Supervision

Caroline West: Conceptualization, Methodology, Resources, Writing – Review & Editing, Vizualization, Supervision, Funding acquisition

References

Abou Baker, D. H., Ibrahim, B. M. M., Hassan, N. S., Yousuf, A. F., & Gengaihi, S. E. (2020). Exploiting Citrus aurantium seeds and their secondary metabolites in the management of Alzheimer disease. *Toxicology Reports*, *7*, 723-729. https://doi.org/10.1016/j.toxrep.2020.06.001

Atwi-Ghaddar, S., Zerwette, L., Destandau, E., & Lesellier, E. (2023). *Supercritical Fluid Extraction (SFE) of Polar Compounds from Camellia sinensis Leaves : Use of Ethanol/Water as a Green Polarity Modifier*.

Bednar, R. A., & Hadcock, J. R. (1988). Purification and characterization of chalcone isomerase from soybeans. *Journal of Biological Chemistry*, *263*(20), 9582-9588. https://doi.org/10.1016/s0021-9258(19)81556-9

Benavente-García, O., & Castillo, J. (2008). Update on Uses and Properties of Citrus Flavonoids : New Findings in Anticancer, Cardiovascular, and Anti-inflammatory Activity. *Journal of Agricultural and Food Chemistry*, *56*(15), 6185-6205. https://doi.org/10.1021/jf8006568

Burbulis, I. E., & Winkel-Shirley, B. (1999). Interactions among enzymes of the *Arabidopsis* flavonoid biosynthetic pathway. *Proceedings of the National Academy of Sciences*, *96*(22), 12929-12934. https://doi.org/10.1073/pnas.96.22.12929

Caccamese, S., Bianca, S., & Santo, D. (2007). Racemization at C-2 of Naringin in Sour Oranges with Increasing Maturity Determined by Chiral High-Performance Liquid Chromatography. *Journal of Agricultural and Food Chemistry*, *55*(10), 3816-3822. https://doi.org/10.1021/jf063355w

Caccamese, S., & Chillemi, R. (2010). Racemization at C-2 of naringin in pummelo (Citrus grandis) with increasing maturity determined by chiral high-

performance liquid chromatography. *Journal of Chromatography A*, *1217*(7), 1089-1093. https://doi.org/10.1016/j.chroma.2009.10.073

Caccamese, S., Manna, L., & Scivoli, G. (2003). Chiral HPLC separation and CD spectra of the C-2 diastereomers of naringin in grapefruit during maturation. *Chirality*, *15*(8), 661-667. https://doi.org/10.1002/chir.10262

Calderaro, A., Patanè, G. T., Tellone, E., Barreca, D., Ficarra, S., Misiti, F., & Laganà, G. (2022). The Neuroprotective Potentiality of Flavonoids on Alzheimer's Disease. *International Journal of Molecular Sciences*, *23*(23), 14835. https://doi.org/10.3390/ijms232314835

Castillo, J., Benavente, O., & del Rio, J. A. (1992). Naringin and Neohesperidin Levels during Development of Leaves, Flower Buds, and Fruits of Citrus aurantium. *PLANT PHYSIOLOGY*, *99*(1), 67-73. https://doi.org/10.1104/pp.99.1.67

Choi, J., Lee, D.-H., Jang, H., Park, S.-Y., & Seol, J.-W. (2020). Naringenin exerts anticancer effects by inducing tumor cell death and inhibiting angiogenesis in malignant melanoma. *International Journal of Medical Sciences*, *17*(18), 3049-3057. https://doi.org/10.7150/ijms.44804

Fugh-Berman, A., & Myers, A. (2004). *Citrus aurantium* , an Ingredient of Dietary Supplements Marketed for Weight Loss : Current Status of Clinical and Basic Research. *Experimental Biology and Medicine*, *229*(8), 698-704. https://doi.org/10.1177/153537020422900802

Gaffield, W., Lundin, R. E., Gentili, B., & Horowitz, R. M. (1975). C-2 stereochemistry of naringin and its relation to taste and biosynthesis in maturing grapefruit. *Bioorganic Chemistry*, *4*(3), 259-269. https://doi.org/10.1016/0045-2068(75)90036-x

Gopal, P. V. (2012). EVALUATION OF ANTI-MICROBIAL ACTIVITY OF CITRUS AURANTIUM AGAINST SOME GRAM POSITIVE AND NEGATIVE BACTERIAL STRAINS. *Pharmacia*, *1*(ISSN 0976-9692), 107-109.

Herrero, M., Cifuentes, A., & Ibañez, E. (2006). Sub- and supercritical fluid extraction of functional ingredients from different natural sources : Plants, food-by-products, algae and microalgae: A review. *Food Chemistry*, *98*(1), 136-148. https://doi.org/10.1016/j.foodchem.2005.05.058

Kang, S. R., Park, K. I., Park, H. S., Lee, D. H., Kim, J. A., Nagappan, A., Kim, E. H., Lee, W. S., Shin, S. C., Park, M. K., Han, D. Y., & Kim, G. S. (2011). Anti-inflammatory effect of flavonoids isolated from Korea Citrus aurantium L. on lipopolysaccharide-induced mouse macrophage RAW 264.7 cells by blocking of nuclear factor-kappa B (NF-κB) and mitogen-activated protein kinase (MAPK) signalling pathways. *Food Chemistry*, *129*(4), 1721-1728. https://doi.org/10.1016/j.foodchem.2011.06.039

Ku, Y.-S., Ng, M.-S., Cheng, S.-S., Lo, A. W.-Y., Xiao, Z., Shin, T.-S., Chung, G., & Lam, H.-M. (2020). Understanding the Composition, Biosynthesis, Accumulation and Transport of Flavonoids in Crops for the Promotion of Crops as Healthy Sources of Flavonoids for Human Consumption. *Nutrients*, *12*(6), 1717. https://doi.org/10.3390/nu12061717

Kumar, S., & Pandey, A. K. (2013). Chemistry and Biological Activities of Flavonoids : An Overview. *The Scientific World Journal*, *2013*, 1-16. https://doi.org/10.1155/2013/162750

Luo, T., He, Y., Jiang, L., Yang, L., Hou, X., Shen, G., Cui, Q., Yu, J., Ke, J., Chen, S., & Zhang, Z. (2025). Flavor perception and biological activities of bitter

compounds in food. *Food Chemistry*, *477*, 143532. https://doi.org/10.1016/j.foodchem.2025.143532

Ma, G., Zhang, L., Yamamoto, R., Kojima, N., Yahata, M., & Kato, M. (2023). Molecular characterization of a flavanone 3-hydroxylase gene from citrus fruit reveals its crucial roles in anthocyanin accumulation. *BMC Plant Biology*, *23*(1). https://doi.org/10.1186/s12870-023-04173-3

Maksoud, S., Abdel-Massih, R. M., Rajha, H. N., Louka, N., Chemat, F., Barba, F. J., & Debs, E. (2021). Citrus aurantium L. Active Constituents, Biological Effects and Extraction Methods. An Updated Review. *Molecules*, *26*(19), 5832. https://doi.org/10.3390/molecules26195832

Martín, J. F., & Liras, P. (2022). Comparative Molecular Mechanisms of Biosynthesis of Naringenin and Related Chalcones in Actinobacteria and Plants : Relevance for the Obtention of Potent Bioactive Metabolites. *Antibiotics*, *11*(1), 82. https://doi.org/10.3390/antibiotics11010082

Molineau, J., Meunier, M., Noireau, A., Fougère, L., Petit, A.-M., & West, C. (2020). Analysis of flavonoids with unified chromatography-electrospray ionization mass spectrometry—Method development and application to compounds of pharmaceutical and cosmetic interest. *Analytical and Bioanalytical Chemistry*, *412*(24), 6595-6609. https://doi.org/10.1007/s00216-020-02798-z

Moulehi, I., Bourgou, S., Ourghemmi, I., & Tounsi, M. S. (2012). Variety and ripening impact on phenolic composition and antioxidant activity of mandarin (Citrus reticulate Blanco) and bitter orange (Citrus aurantium L.) seeds extracts. *Industrial Crops and Products*, *39*, 74-80. https://doi.org/10.1016/j.indcrop.2012.02.013

Ni, R., Zhu, T.-T., Zhang, X.-S., Wang, P.-Y., Sun, C.-J., Qiao, Y.-N., Lou, H.-X., & Cheng, A.-X. (2020). Identification and evolutionary analysis of chalcone isomerase-fold proteins in ferns. *Journal of Experimental Botany*, *71*(1), 290-304. https://doi.org/10.1093/jxb/erz425

Okamoto, D., & Hirata, Y. (2006). Development of Supercritical Fluid Extraction Coupled to Comprehensive Two-dimensional Supercritical Fluid Chromatography (SFE-SFC×SFC). *Analytical Sciences*, *22*(11), 1437-1440. https://doi.org/10.2116/analsci.22.1437

Pirok, B. W. J., Stoll, D. R., & Schoenmakers, P. J. (2019). Recent Developments in Two-Dimensional Liquid Chromatography : Fundamental Improvements for Practical Applications. *Analytical Chemistry*, *91*(1), 240-263. https://doi.org/10.1021/acs.analchem.8b04841

Ren, W., Qiao, Z., Wang, H., Zhu, L., & Zhang, L. (2003). Flavonoids : Promising anticancer agents. *Medicinal Research Reviews*, *23*(4), 519-534. https://doi.org/10.1002/med.10033

Réset, L., De Saint Jores, C., François, I., & West, C. (2024). Development of a Two-Dimensional Supercritical Fluid Chromatography System in Multiple Heart-Cutting Modes. *Analytical Chemistry*, *96*(29), 11969-11976. https://doi.org/10.1021/acs.analchem.4c01795

Réset, L., De Saint Jores, C., & West, C. (2024). Chiral and achiral analysis of chiral flavonoids with liquid and supercritical fluid chromatography – A review. *Journal of Chromatography Open*, *6*, 100183. https://doi.org/10.1016/j.jcoa.2024.100183

Sánchez-Camargo Andrea del Pilar, Parada-Alfonso Fabián, Ibáñez Elena, & Cifuentes Alejandro. (2016). On-line coupling of supercritical fluid extraction

and chromatographic techniques. *Journal of Separation Science*, *40*(1), 213-227. https://doi.org/10.1002/jssc.201601040

Shen, C.-Y., Jiang, J.-G., Huang, C.-L., Zhu, W., & Zheng, C.-Y. (2017). Polyphenols from Blossoms of *Citrus aurantium* L. var. *Amara* Engl. Show Significant Anti-Complement and Anti-Inflammatory Effects. *Journal of Agricultural and Food Chemistry*, *65*(41), 9061-9068. https://doi.org/10.1021/acs.jafc.7b03759

Suntar, I., Khan, H., Patel, S., Celano, R., & Rastrelli, L. (2018). An Overview on *Citrus aurantium* L. : Its Functions as Food Ingredient and Therapeutic Agent. *Oxidative Medicine and Cellular Longevity*, *2018*(1), 7864269. https://doi.org/10.1155/2018/7864269

Testai, L., & Calderone, V. (2017). Nutraceutical Value of Citrus Flavanones and Their Implications in Cardiovascular Disease. *Nutrients*, *9*(5), 502. https://doi.org/10.3390/nu9050502

Tungmunnithum, D., Thongboonyou, A., Pholboon, A., & Yangsabai, A. (2018). Flavonoids and Other Phenolic Compounds from Medicinal Plants for Pharmaceutical and Medical Aspects : An Overview. *Medicines*, *5*(3), 93. https://doi.org/10.3390/medicines5030093

West, C. (2018). Current trends in supercritical fluid chromatography. *Analytical and Bioanalytical Chemistry*, *410*(25), 6441-6457. https://doi.org/10.1007/s00216-018-1267-4

West, C. (2019). Recent trends in chiral supercritical fluid chromatography. *TrAC Trends in Analytical Chemistry*, *120*, 115648. https://doi.org/10.1016/j.trac.2019.115648

West, C., Melin, J., Ansouri, H., & Mengue Metogo, M. (2017). Unravelling the effects of mobile phase additives in supercritical fluid chromatography. Part I : Polarity

and acidity of the mobile phase. *Journal of Chromatography A*, *1492*, 136-143. https://doi.org/10.1016/j.chroma.2017.02.066

Wistuba, D., Trapp, O., Gel-Moreto, N., Galensa, R., & Schurig, V. (2006). Stereoisomeric Separation of Flavanones and Flavanone-7-*O*-glycosides by Capillary Electrophoresis and Determination of Interconversion Barriers. *Analytical Chemistry*, *78*(10), 3424-3433. https://doi.org/10.1021/ac0600499

Zhang, C., Liu, Y., Liu, X., Chen, X., & Chen, R. (2023). Comprehensive Review of Recent Advances in Chiral A-Ring Flavonoid Containing Compounds : Structure, Bioactivities, and Synthesis. *Molecules*, *28*(1), 365. https://doi.org/10.3390/molecules28010365

Zou, Z., Xi, W., Hu, Y., Nie, C., & Zhou, Z. (2016). Antioxidant activity of Citrus fruits. *Food Chemistry*, *196*, 885-896. https://doi.org/10.1016/j.foodchem.2015.09.072

Supplementary information to:

Determination of the diastereomeric excesses of chiral flavonoids in organs of *Citrus aurantium* with two-dimensional supercritical fluid chromatography

Laurine Réset, Bibi Ousseni, Laetitia Fougère, Christophe Hano, Clément De Saint Jores, Caroline West*
Université d'Orléans, CNRS, ICOA, UMR 7311, Orléans, France

Table S1. Three factors and levels in the Box-Behnken design of experiments (DoE) used to optimize extraction. Oven temperature (T), total percentage of co-solvent (C) and water percentage introduced in the co-solvent (W), with three levels coded as (+1) highest level, (0) middle level and (-1) lowest level. See Table S1 in supplementary information for detailed experiments.

Factors	levels		
	-1	**0**	**1**
T (°C)	40	60	80
C (%)	10	20	30
W (%)	0	10	20

Table S2. Box-Behnken design of experiments to optimize SFE conditions. T is the oven temperature, C is the percentage of co-solvent introduced in pressurized CO_2, W is the percentage of water in the ethanol co-solvent. Although the table is organized in this view, it was randomized before doing the experiments.

#	T (°C)	C (%)	W (%)
1	-1	-1	0
2	1	-1	0
3	-1	1	0
4	1	1	0
5	-1	0	-1
6	1	0	-1
7	-1	0	1
8	1	0	1
9	0	-1	-1
10	0	1	-1
11	0	-1	1
12	0	1	1
13	0	0	0
14	0	0	0
15	0	0	0
16	0	0	0
17	0	0	0

Figure S1. Representation of 13 experimental conditions tested in the Box-Behnken design. The central point was repeated 5 times.

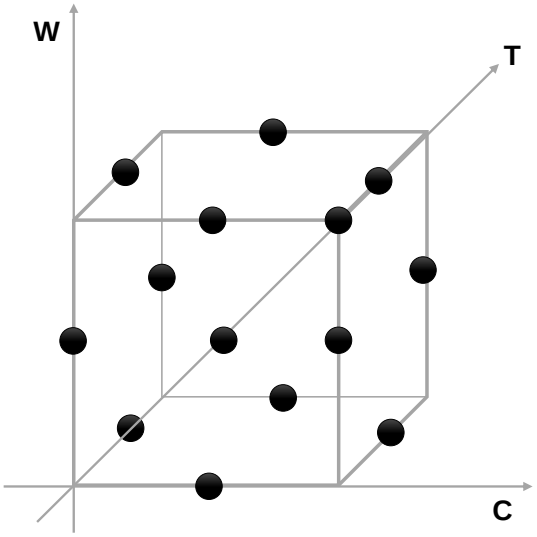

Figure S2. Significant terms in the quadratic models established for the total extracted mass and the neohesperidin peak area, based on the 17 experiments in the Box-Behnken design.

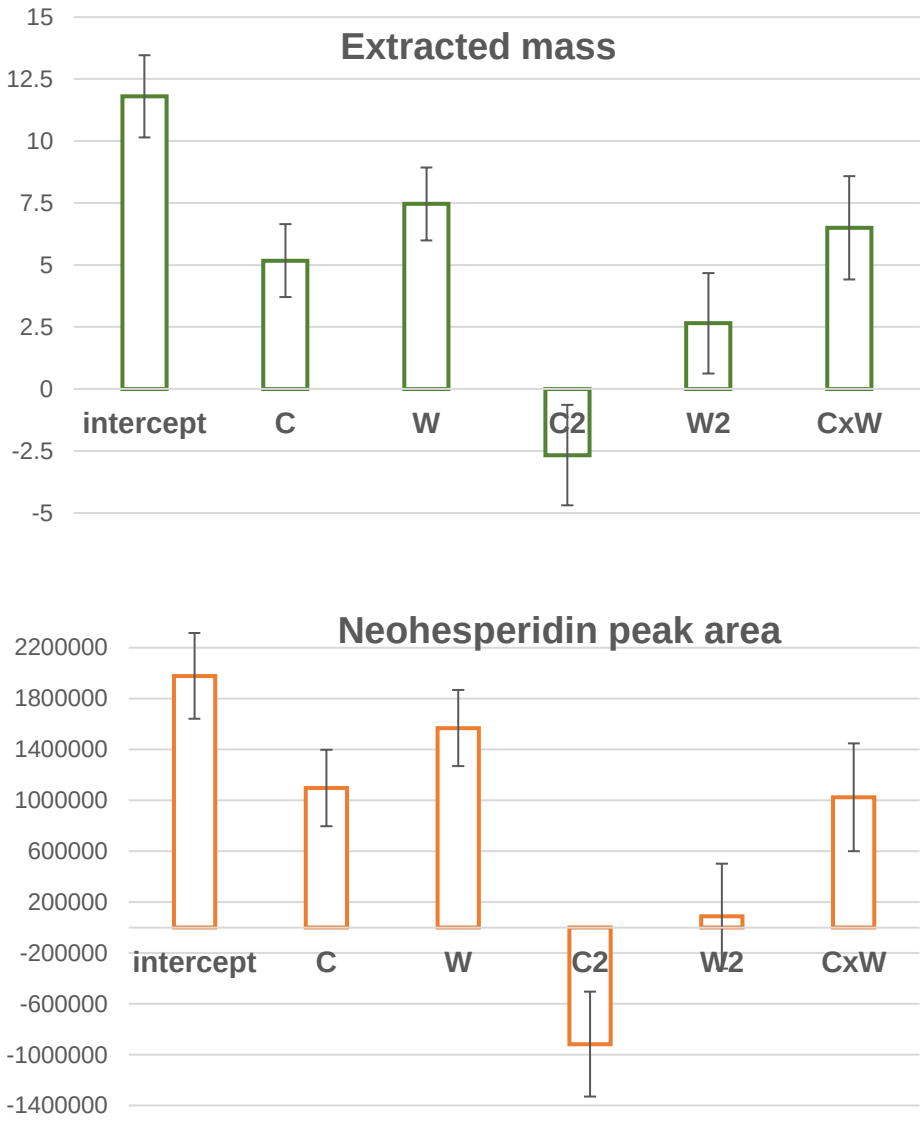

Figure S3. Response curves observed for the total extracted mass and peak area of neohesperidin, based on the quadratic models in Figure S2, and depending on the percentage of co-solvent introduced in pressurized CO_2 (C) and the percentage of water introduced in ethanol co-solvent (W).

Extracted mass

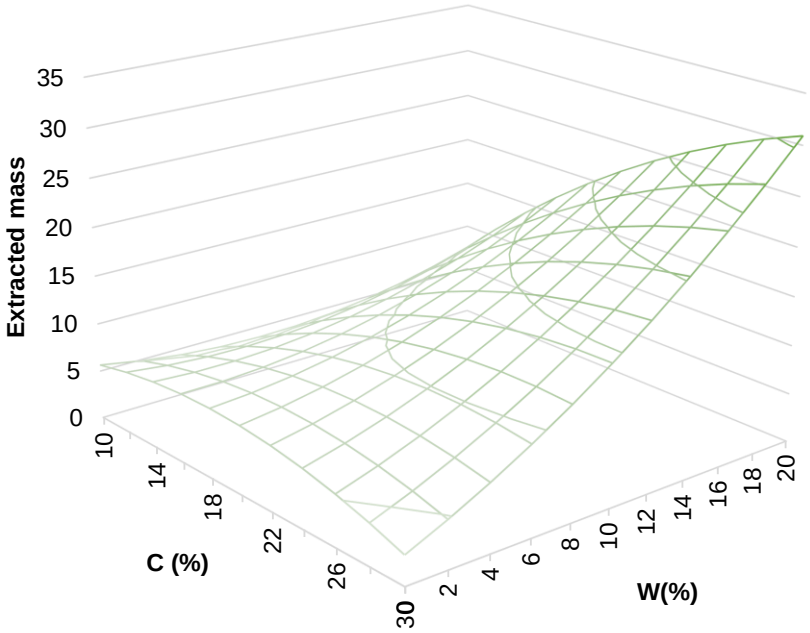

Neohesperidin peak area

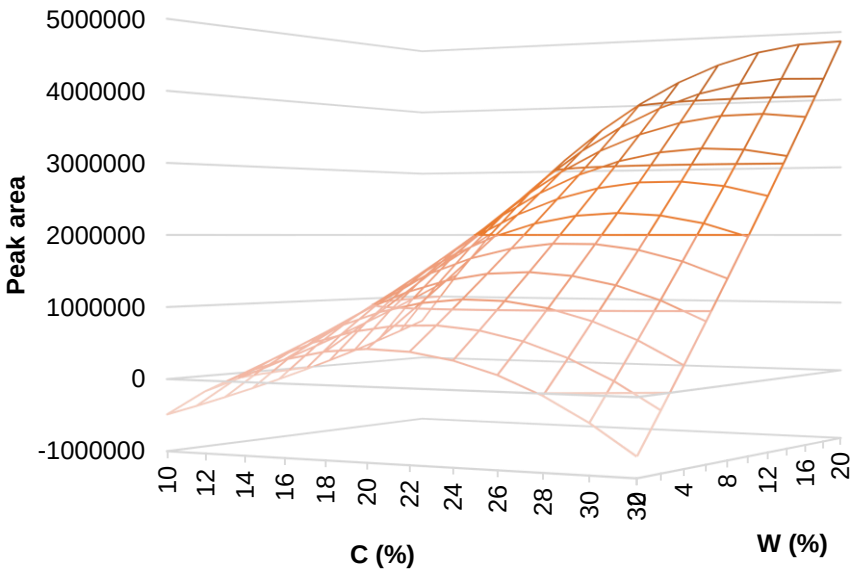

Table S3. Gradient profiles in the two dimensions of the SFC-SFC method.

Time (min)	Co-solvent (%)	Back-pressure (bar)	Flow rate (mL/min)
a. First-dimension method			
0.0	20	150	1.7
0.5	20	150	1.7
8.0	100	110	0.6
10.0	100	110	0.6
10.5	20	110	0.6
12.0	20	150	1.7
12.5	20	150	1.7
b. Second-dimension method			
0.0	15	150	2.0
0.5	15		
17.0	50		
19.0	50		
19.5	15		
22.0	15		

Figure S4. 6-day stability study of the d.e. of neohesperidin (A) and naringin (B) in an orange peel sample (blue) and in standards (purple).
SFC-SFC analysis conditions are identical to Figure 2.

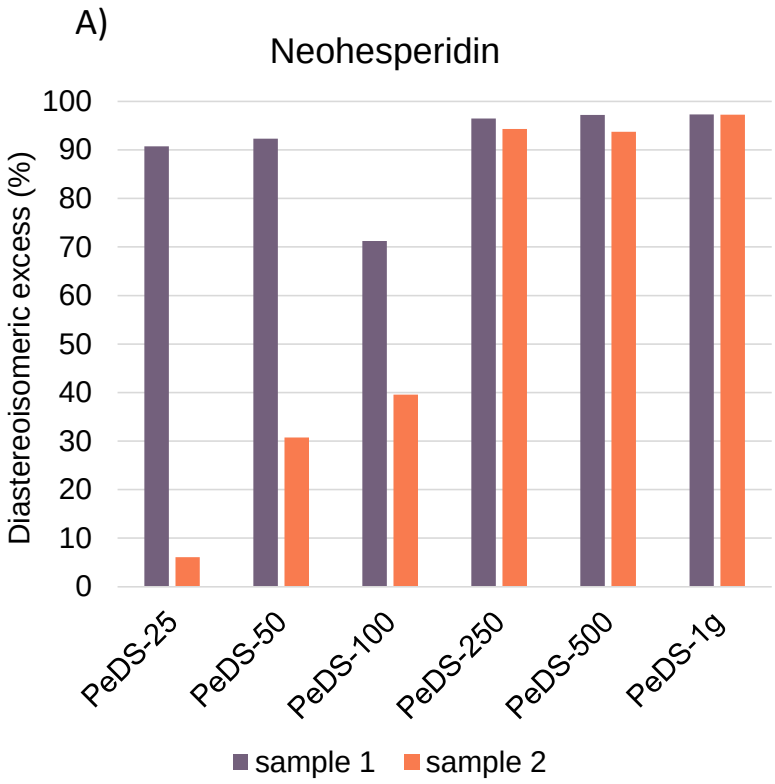

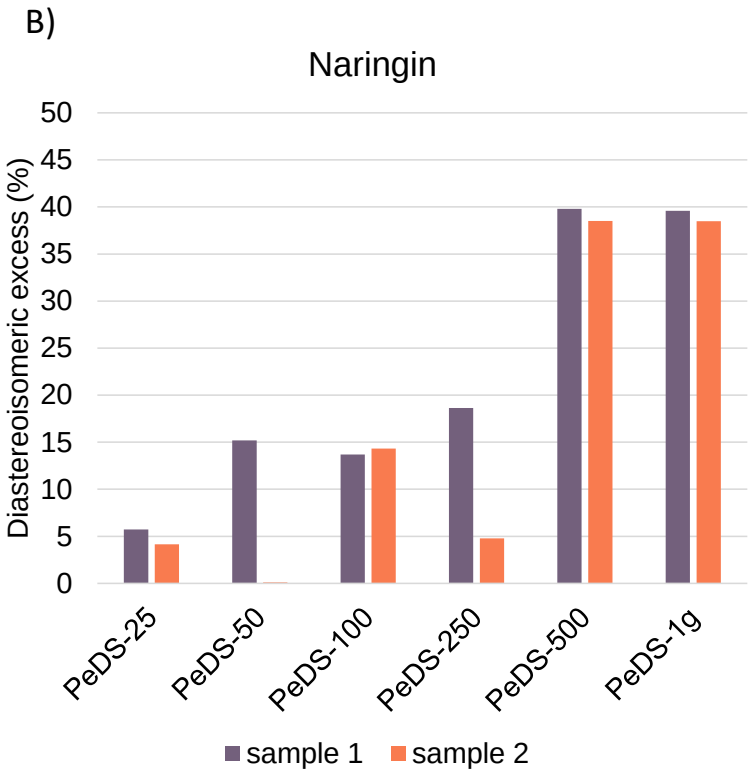

Figure S5 – Comparison of the d.e. values of neohesperidin (purple) and naringin (orange) for samples of ripe orange peel with different drying methods (lyophylisation, oven and unknown drying conditions for the commercial sample from Louis Hesboristerie). SFC-SFC analysis conditions are identical to Figure 2.